

Numerical Simulation of the Laval Annular Mechanical Foam Breaker for Foam Drilling

Pin Lu Cao, Jinsong Wang, Chun Peng Liu and Rusheng Wang
College of Construction Engineering, Jilin University, Changchun 130061, China

Abstract: The Computational Fluid Dynamics (CFD) code, Fluent, is employed to simulate the flow phenomena inside the annular foam breaker in order to improve its performance. The numerical simulation results show that the value and the distribution of the negative pressure are very important for the annular foam breaker. The design of the Laval nozzle not only can increase the fluid velocity, but also can reduce the pressure value from -30.2 to -50.3 kPa compared with the common annular nozzle foam breaker. In order to improve the range of the internal negative pressure, the two-stage Laval annular foam breaker is designed in this study. The analysis results show the distance between the two annular slit have greatly influence on its performance. There is a small overlap area between the two negative pressure zones generated by the two annular slits. The smaller the value distance is, the larger the overlap zone is. When the value of the distance decreases to 50 mm, the minimum negative pressure can be reduced to approximately -65.5 kPa. Meanwhile, the range of the internal negative pressure is larger than the single Laval annular foam breaker, which is benefit to break foam.

Keywords: Annular foam breaker, CFD analysis, coanda effect, foam drilling, laval nozzle

INTRODUCTION

Though air foam drilling technology has been widely used in drilling oil and gas wells, which has proved its efficiency in numerous situations where serious problems were encountered such as in fractured formations and depleted or high permeable zones, the main challenge is that after returning to the surface the foam remains stable and requires a long period of time to dissipate back to the volume of the original liquid (Teichrob and Manuel, 1997; Cao *et al.*, 2009). Not only is an extremely large pit required to contain the foam, but also the foam liquid can be used only once since it cannot be broken down fast enough. So it needs enormous volume prepared foam liquid, consumes abundance of water and ingredient additives, which greatly increased the drilling cost. Moreover, amount of foams accumulated in mud pit will be blown out easily with wind, carrying various chemicals which result in environment pollution (Song *et al.*, 1998; Liu *et al.*, 2006).

Both chemical and mechanical methods are available for foam breaking (Morey *et al.*, 1999; Neethling *et al.*, 2003; Hamilton *et al.*, 1991). Mechanical foam breaker is preferable to chemical methods, avoiding problems such as changing the chemical and physical properties of the foam system which pollute the foam surfactant and reduce its foamability that the foam drilling fluid cannot be reused, or adverse effects on environment seen when foaming is controlled by the addition of antifoam agents (Pelton, 2002). A number of mechanical foam breakers

have so far been proposed including high rotate centrifugal foam breaker (Vetoshkin, 2003), foam-breaking cyclones (Guzman, 2005) and air jet breaker (Vetoshkin and Chagin, 2002), etc., (Satoshi *et al.*, 2003; Takesono *et al.*, 2006; Zagorskina and Sokovnin, 2001; Barigou, 2001; Satoshi *et al.*, 2007; Deshpande and Barigou, 2000). However, most of these breakers are hardly practical for foam-breaking operation in high-rate gas bubbling systems of foam drilling fluid. Designing effective and economical mechanical foam breakers become necessary.

Previously, the annular mechanical foam breaker designed mainly based on Coanda effect has been developed and tested in field (Hazaea *et al.*, 2007). Though it has been successful applied to foam drilling and the foam solution can be really recycled and reutilized, the foam-breaking efficiency of the annular foam breaker is not stable. If foaming is too excessive, or the liquid phase viscosity is too high, the annular foam breaker will be ineffective (Cao *et al.*, 2012a). We should by noting that, the annular foam breaker mainly uses vacuums produced by Coanda effect to destroy foam. In other words, the high speed air-stream emerging from an annular nozzle tends to follow nearby curved surfaces thanks to the Coanda effect, if the curvature of the surface or angle that the surface makes with the stream is not too sharp, which causes the pressure nearby decrease. When the foam drilling fluid flow through this low pressure region, the bubble will be burst as a result of quickly changed in pressure. Therefore, the vacuum value and the pressure distribution inside the annular foam breaker have great

influence on its efficiency. In order to develop an annular foam breaker with high performance, it is very important to improve the pressure distribution inside it.

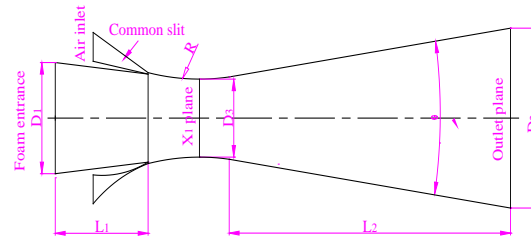
In this study, the new type of annular foam breaker with two Laval annular slits is designed. The various flow patterns inside the annular foam breaker are analyzed using a commercial CFD code FLUENT with a Preprocessor, GAMBIT. For contrast, the flow characteristic of the common annular foam breaker with one slit is also simulated using CFD method.

THE FLOW CHARACTERISTIC OF THE LAVAL ANNULAR FOAM BREAKER

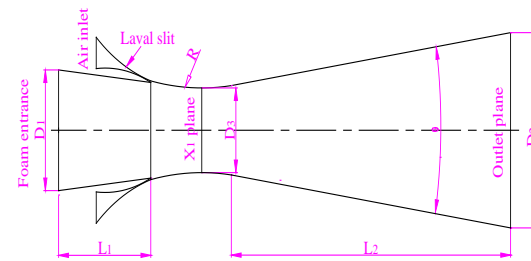
Analytical models: CFD commercial package, FLUENT6.0, has been used to conduct the numerical analysis on the annular foam breaker. Since the annular foam breaker are axisymmetric as shown in Fig. 1, a 2D axisymmetric model has been created with a structured grid system with quadrilateral mesh element in order to reduce computer costs and data manipulation time. The dense meshes are preset at the area of high flow rate and high pressure gradient so as to obtain accurate results. For an axisymmetric turbulent compressible flow, the governing equations of continuity, momentum and energy are solved simultaneously with the constraint, the ideal gas law. The standard k- ϵ model is selected to model the turbulent viscosity with applying coupled-implicit solver. The near wall treatment is left as the standard wall function, which give reasonably accurate results for the wall bounded with very high Reynolds number flow.

According to the optimization results of the common annular foam breaker, the structural parameters used in this study are as follows: $L_1 = 70$ mm, $D_1 = 80$ mm, $R = 100$ mm, $D_3 = 60$ mm, $L_2 = 400$ mm, $\theta = 8^\circ$, where L_2 is the length of the diffuser; R is the radius of the Coanda surface; D_1 , D_2 and D_3 are the diameters of the foam entrance plane, the exit plane of diffuser and the throat plane of the foam breaker, respectively; θ is the diffuser angle (Cao *et al.*, 2012b). The only difference between the common annular foam breaker and the Laval ones is the shape of the annular slit, as shown as in Fig. 1.

Figure 2 illustrates the boundary conditions for numerical analysis. The mass flow inlet and the pressure inlet are applied to the boundary of the air channel and the foam entrance, respectively. The initial mass flow rate at the inlet is about 0.10 kg/s. Since the foam burst process is very complicated and difficult to simulate, the pressure inlet boundary is set to atmospheric conditions to simplify the calculation. The boundary condition at the exit of the annular foam breaker has been chosen to be pressure outlet condition with atmospheric pressure. In this study, all the walls are considered to be adiabatic with no slip.



(a) The common annular foam breaker



(b) The laval annular foam breaker

Fig. 1: The analytical models of the annular foam breaker

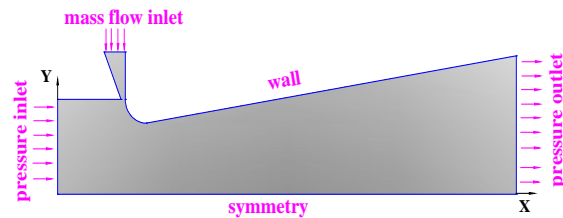
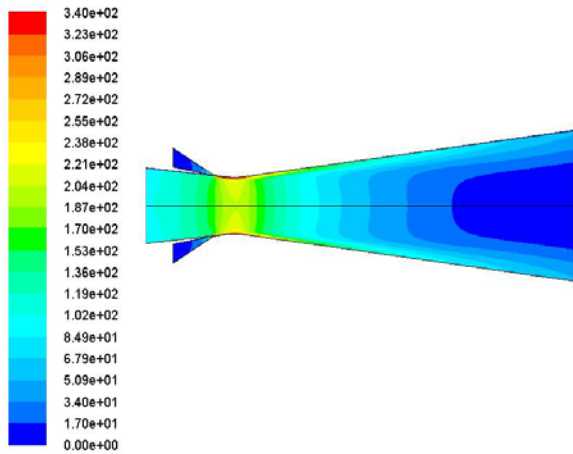


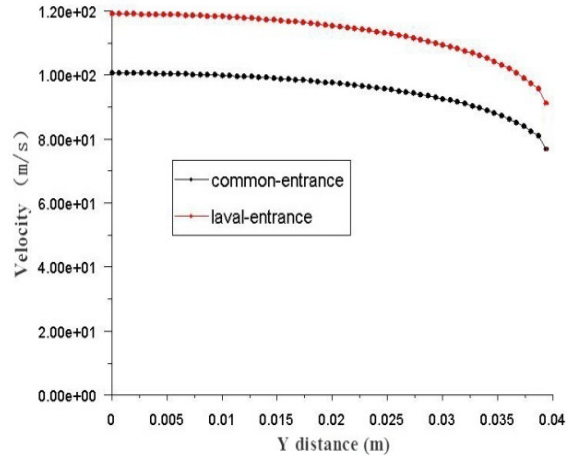
Fig. 2: The boundary conditions of the annular foam breaker

Results and discussion: Figure 3 shows the velocity distribution contours inside the annular foam breaker. The velocity field distribution inside the Laval foam breaker is almost the same as that in common foam breaker. The air-stream flows through the annular slits at a high speed and adheres to the Coanda surface and the wall of the diffuser.

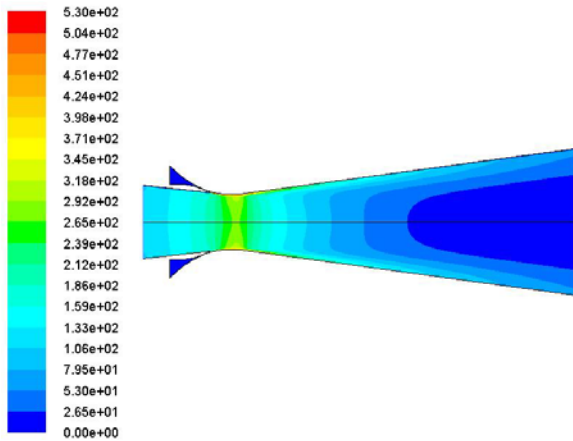
This high speed jet induces the ambient air near the entrance flow into the foam breaker, as can be seen from Fig. 4a. On the other hand, the high speed jet interacts with the relatively low speed induced flow and mix all along the length of the foam breaker. The difference in velocity between the jet and the induced flow makes the momentum transfer from the high velocity air stream to induced flow, which accelerates the induce flow as shown in Fig. 4b. On close observation of the velocity profiles at the X1 plane (the throat plane of the annular foam breaker), it may be seen that the graph can be split into two parts: the first part characterized by large gradient with high velocities and a second part where the velocity gradient is small. The first part represents the jet coming through the annular nozzle while the second part is related to the



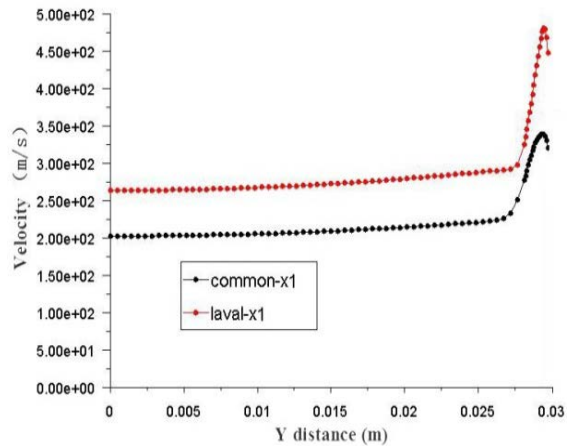
(a) The common annular foam breaker



(a) Velocity profiles at foam entrance plane



(b) The laval annular foam breaker



(b) Velocity profiles at X_1 plane

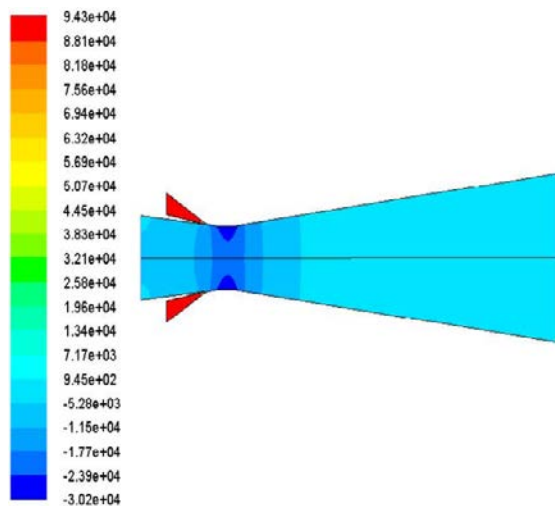
Fig. 3: Velocity contours inside the annular foam breaker (m/s)

Fig. 4: Velocity distribution inside the annular foam breaker at different planes

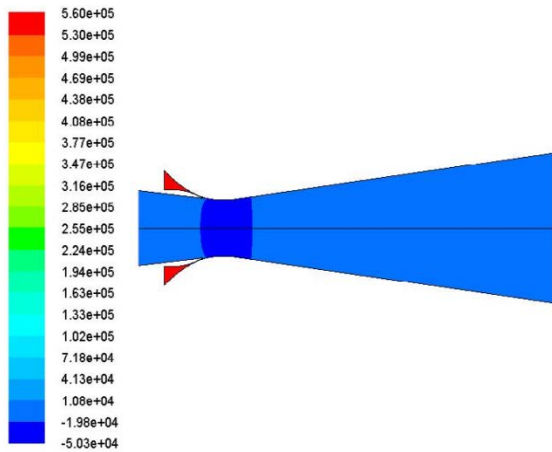
induced flow. Moreover, a stronger shear force will be generated in the process of the momentum transfer between the jet and the induced flow, which will destroy the bubbles if the induced flow is replaced by foam fluid.

The static pressure distribution contours inside the annular foam breaker are shown in Fig. 5. We can see that the local static pressure of the fast moving air stream will be less than ambient pressure. The lowest pressure is about -50.3 kPa for the Laval foam breaker, which is located at the throat plane nearby the Coanda surface, while it is about -30.2 kPa for the common one located at the same region. If the foam fluid flows through this negative pressure region, it will be bursted under the effect of the pressure difference.

Figure 6 shows comparisons of the static pressure profiles of the two foam breakers at the same plane locations. It can be seen that the static pressure profiles are smaller in magnitude for the Laval annular foam

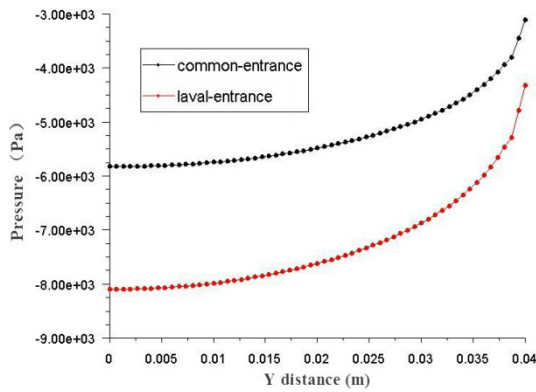


(a) The common annular foam breaker

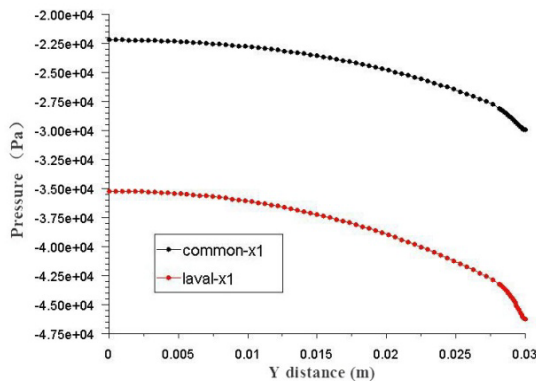


(b) The laval annular foam breaker

Fig. 5: Static pressure contours inside the annular foam breaker (Pa)



(a) Pressure profiles at foam entrance plane



(b) Pressure profiles at X_1 plane

Fig. 6: Pressure distribution inside the annular foam breaker at different planes

breaker than for the common annular foam breaker at all planes. The static pressure reaches a minimum near the wall and then rapidly increases to a uniform value in

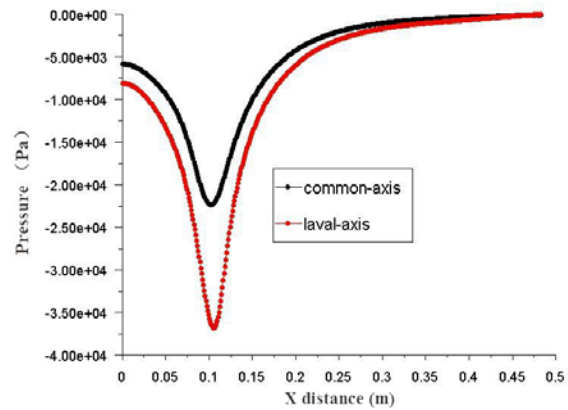


Fig. 7: Pressure distribution along the axis of the annular foam breaker ($y = 0$)

the center of the foam breaker for both annular foam breakers. The lowest pressure near the wall at X_1 plane is closed to -47 kPa in the Laval annular foam breaker, while it is no more than -30 kPa in the common annular foam breaker as shown in Fig. 6b.

Figure 7 illustrates the static pressure distributions along the axis of the annular foam breaker. It is found that the pressure decreases rapidly to a negative value near the throat and then gradually recovers along the diffuser to ambient pressure for both foam breakers. The lowest pressure value along the axis of the Laval annular foam breaker is reduced from -22 to -37 kPa compared with the common annular foam breaker as depicted in Fig. 7.

Based on above analysis, we can draw a conclusion that the jet momentum of the Laval annular foam breaker is bigger and the vacuum degree inside it is higher than those of the common one at the same conditions, which are benefit to breaking foam fluid. Therefore, the performance of the Laval annular foam breaker is better than the common one.

However, whether the Laval annular foam breaker or the common one, the negative pressure is generated only in the vicinity of the annular slit. The range of the negative pressure is so narrow that some bubbles may have no enough time to burst if the foam velocity is too fast or the liquid phase viscosity is too high. That is the main reason why the annular foam breaker sometimes is not so effective. Thus it is very important to increase the negative pressure range to improve the performance of the annular foam breaker.

THE FLOW CHARACTERISTIC OF THE TWO-STAGE LAVAL ANNULAR FOAM BREAKER

Analytical models: Keeping the structural parameters unchanged, the second annular slit is designed in the diffuser of the Laval annular foam breaker expecting to increase the internal negative pressure range by adding another annular slit, named as the two-stage Laval

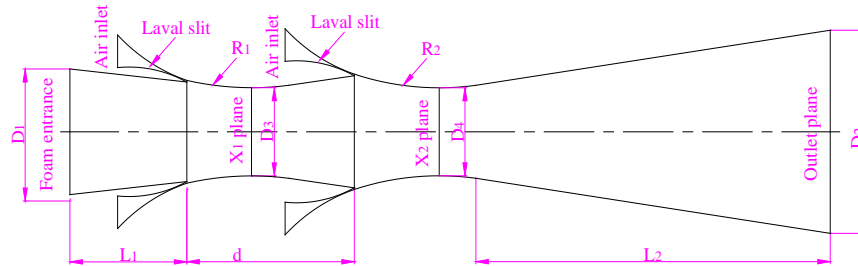


Fig. 8: The analytical model of the two-stage laval annular foam breaker

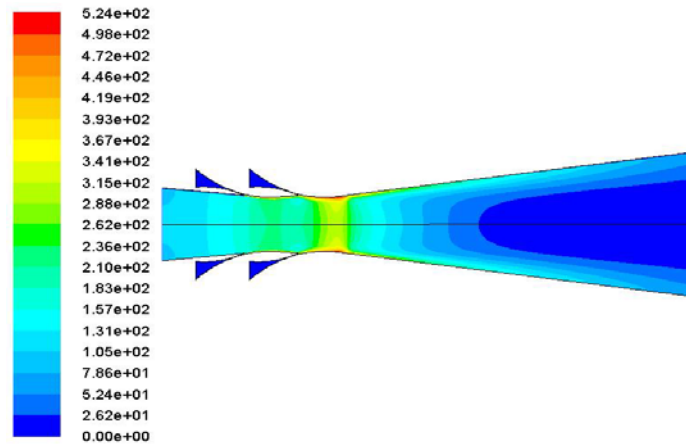


Fig. 9: Velocity distribution contours inside the two-stage annular foam breaker (m/s)

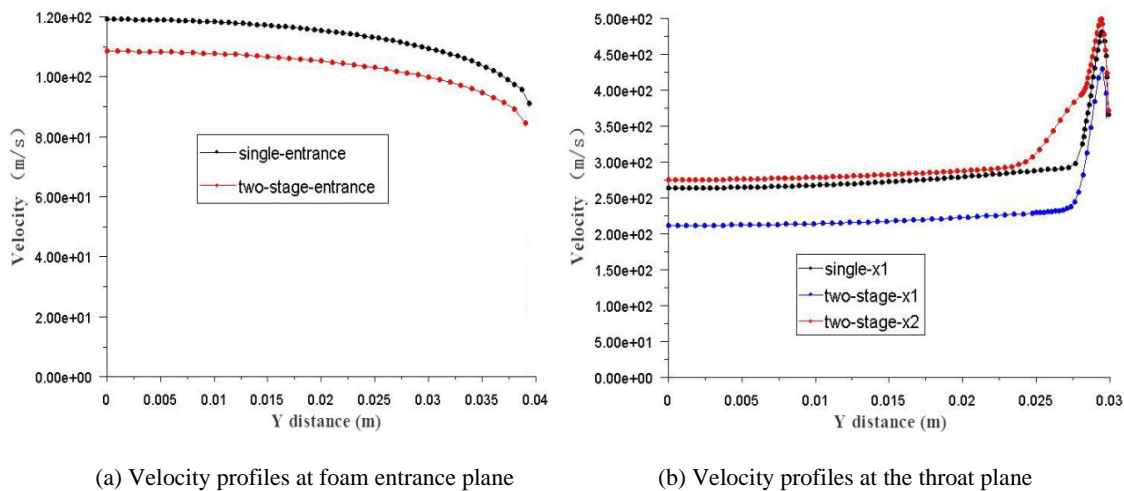


Fig. 10: Comparison of velocity profiles for different annular foam breaker

annular foam breaker as shown in Fig. 8. The size and shape of the second nozzle are the same as that of the first one. That is to say, $R_1 = R_2$ and $D_3 = D_4$. Keeping the distance d between two Laval nozzles as 50 mm, the flow field of the two-stage Laval annular foam breaker is analyzed using commercial CFD software, FLUENT. An axial symmetric model is again used. The mass flow inlet is applied to the boundary of the air channel. And the initial mass flow rate is about 0.10 kg/s for both air

inlets. The pressure inlet and the pressure outlet are applied to the boundary of the foam entrance and the diffuser outlet, respectively.

RESULTS AND DISCUSSION

The velocity distribution contours inside the two-stage Laval annular foam breaker are given in Fig. 9. As mentioned before section, the high speed jet

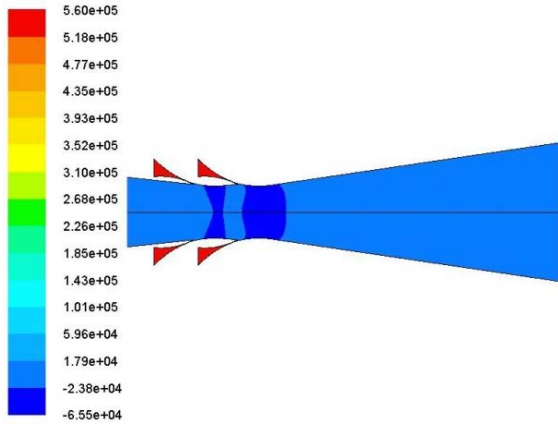


Fig. 11: Static pressure contours inside the foam breaker (Pa)

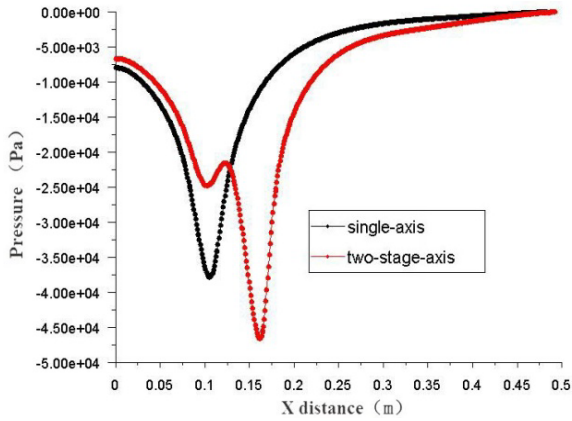


Fig. 12: Pressure distributions along the axis of the foam breaker

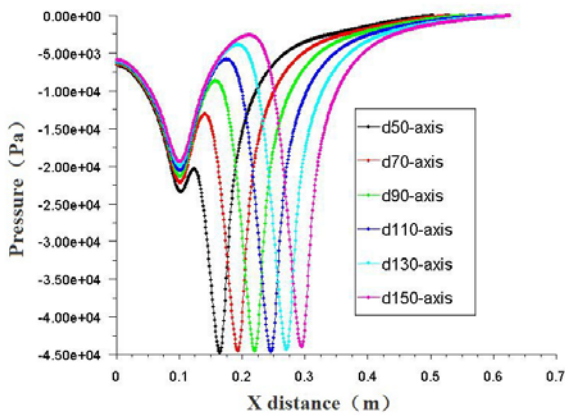


Fig. 13: Pressure profiles for various "d"

coming from the first Laval annular slit adheres to the arc surface due to the Coanda effect and creates within the restriction at this intermediate conduit region a violent sucking in the ambient air near the foam entrance. The high speed air stream mixed with the induced flow advances through the diffuser and arrives

at the arc surface of the second annular slit. Here they meet with another high speed flow ejecting from the second annular slit, then continue to move forward together. Moreover, we can see that the maximum velocity is found around the arc surface of the second annular slit since the flow flows along the curvature surface by Coanda effect.

Figure 10 shows comparisons of the velocity profiles between the single and the two-stage Laval annular foam breaker. The initial velocity of the induced flow at the foam entrance plane is smaller in magnitude for the two-stage Laval annular foam breaker than the single one as described in Fig. 10a. The same trend can be observed at the throat plane X1. But the velocity of the two-stage annular foam breaker at the second throat plane X2 is slightly larger than the velocity of the single foam breaker at the throat plane X1.

It can be seen from Fig. 11 that the negative pressure is generated in nearby each Coanda surface. And any decrease in static pressure will result in the liberation of gas bubbles. Compared with the single Laval annular foam breaker, the minimum pressure is reduced from -50.3 to -65.5 kPa.

Figure 12 shows the static pressure distributions along the axis of the two-stage Laval annular foam breaker. The pressure decreases rapidly from the foam entrance to the throat plane X1, after a short slightly rising, it is reduced quickly to the minimum at the throat plane X2. Then the pressure begins to recover gradually along the diffuser to ambient pressure. As expected, the negative pressure range is improved greatly compared with the single Laval annular foam breaker as shown in Fig. 12.

The distance between the two annular slit, termed as "d", undoubtedly has a great effect on the internal pressure distribution of the two-stage Laval annular foam breaker. Keeping the other parameters unchanged, different d values has been investigated using CFD code, Fluent. The calculation results are given in Fig. 13. It can be seen that there is a small overlap between the two negative pressure zones. The larger the value distance d is, the smaller the overlap zone of the negative pressure is. When the value of the distance increases to 150 mm, the pressure between the two negative pressure zones is almost recovery to normal pressure, which is unfavorable for foam breaking. In order to provide the convenience for manufacturing process, the value d advised here is 50 mm.

CONCLUSION

The structure of the annular foam breaker is very simple and there is no moving parts or small openings that could plug during service. It turns out to be one of the most effective ways since it combines two effects of vacuum and shear force to break foam. The flow characteristics inside the annular foam breaker are numerically simulated in order to further improve its

performance using CFD software Fluent. Based on the results obtained in the present work, the following conclusions can be drawn:

A stream of air at high velocity attached to a curved surface causes a low pressure region nearby, which results in foam-breaking. So the negative pressure distribution has a strong influence on the performance of the annular foam breaker.

The design of the Laval nozzle is not only helpful to increase the fluid velocity, but also can decrease the pressure value. The minimum pressure can be reduced from -30.2 to -50.3 kPa compared with the common annular foam breaker.

The distance between the two annular slit have greatly influence on its performance for the two-stage Laval annular foam breaker designed in this study. The minimum pressure has reached about -65.5 kPa when the distance is 50 mm. At the same time, the range of the internal negative pressure is larger than the single Laval annular foam breaker, which is benefit to break foam.

It is preferable to use the two-stage Laval annular foam breaker to break foam drilling fluid. However its actual effect needs to be verified by the experiment.

ACKNOWLEDGMENT

The research presented in this study was supported by the basic research fund of Jilin University (No. 201003037) and China Petroleum and Chemical Corporation (No. SG10032).

REFERENCES

- Barigou, M., 2001. Foam rupture by mechanical vibrational methods. *Chem. Eng. Technol.*, 24(6): 659-663.
- Cao, P.L., J.C. Zhang, X. Wu and J.Y. Huang, 2009. Research and development on foam breaking and recycling technology in ai-foam drilling. *Global Geol.*, 12(4): 204-209.
- Cao, P.L., Z.Y. Hu, B.Y. Chen, Z.C. Zheng and W.Y. Ma, 2012a. Experiment and application of an annular foam breaker for foam drilling fluid. *Int. J. Eng. Trans. B: Appl.*, 25(1): 73-79.
- Cao, P.L., B.Y. Chen, Z.C. Zheng and W.Y. Ma, 2012b. Numerical simulation and optimization design of the annular mechanical foam breaker. *Int. J. Eng. Trans. C: Aspects*, 25(2): 111-118.
- Deshpande, N.S. and M. Barigou, 2000. Mechanical suppression of the dynamic foam head in bubble column reactors. *Chem. Eng. Process.*, 39(3): 207-217.
- Guzman, N.M., 2005. Foam flow in gas-liquid cylindrical cyclone compact separator. Ph.D. Thesis, University of Tulsa, pp: 59-61.
- Hamilton, B.E., B.K. Moore and D.E. Newton, 1991. Foam Breaker and Method. United States Patent, US 5015273.
- Hazaea, M., Y.H. Sun, O.E.H. Yarbana, L.X. Xu and A.A. Fahmi, 2007. Research on experiment and calculation of foam bursting device. *Global Geol.*, 10(1): 34-38.
- Liu, D.S., Z.H. Li and X.L. Liu, 2006. Recovery and reuse of air-foam drilling fluid. *Drill. Fluid Completion Fluid*, 23(1): 11-14, (In Chinese).
- Morey, M.D., N.S. Deshpande and M. Barigou, 1999. Foam destabilization by mechanical and ultrasonic vibrations. *J. Colloid Interf. Sci.*, 219(1): 90-98.
- Neethling, S.J., H.T. Lee and J.J. Cilliers, 2003. Simple relationships for predicting the recovery of liquid from flowing foams and froths. *Minerals Eng.*, 16(11): 1123-1130.
- Pelton, R., 2002. A review of antifoam mechanisms in fermentation. *J. Ind. Microbiol. Biotechnol.*, 29(4): 149-154.
- Satoshi, T., O. Masayuki, Y. Masanori, Y. Kazuaki and O. Akira, 2003. Performance characteristics of mechanical foam-breakers fitted to a stirred-tank reactor. *J. Chem. Technol. Biot.*, 78(1): 48-55.
- Satoshi, T., O. Masayuki, Y. Masanori, Y. Kazuaki and O. Akira, 2007. Foam breaking characteristics of a mechanical foam-breaker using shear force fitted to a stirred-tank reactor. *J. Chem. Eng. Jpn.*, 40(7): 565-570.
- Song, J.S., S.X. Ou, Z.M. Shan and G.Q. Zhang, 1998. Application of circulation foam drilling technology. *Oil Drill. Prod. Technol.*, 20(6): 24-28, (In Chinese).
- Takesono, S., M. Onodera, K. Toda, M. Yoshida, K. Yamagiwa and A. Ohkawa, 2006. Improvement of foam breaking and oxygen-transfer performance in a stirred-tank fermenter. *Bioprocess Biosyst. Eng.*, 28(4): 235-242.
- Teichrob, R.R. and J.J. Manuel, 1997. Underbalanced foam drilling reduces whole problems and costs. *Oil Gas J.*, 95(33): 52-55.
- Vetoshkin, A.G., 2003. Modeling of centrifugal rotary plate foam breakers. *Theor. Found. Chem. Eng.*, 37(4): 372-377.
- Vetoshkin, A.G. and B.A. Chagin, 2002. Analysis of operating conditions for an aerodynamic foam breaker. *Theor. Found. Chem. Eng.*, 36(2): 113-117.
- Zagoskina, N.V. and O.M. Sokovnin, 2001. Conditions for foam flow and breaking. *Theor. Found. Chem. Eng.*, 35(1): 95-98.